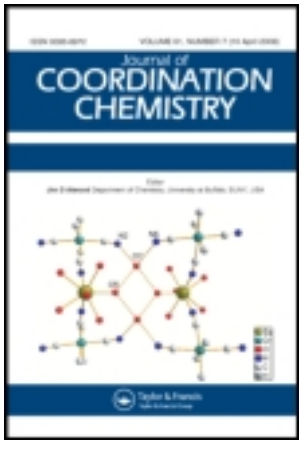

Journal of Coordination Chemistry
Publication details, including instructions for authors and subscription information:
http://www.tandfonline.com/loi/gcoo20

Synthesis, characterization, electrochemical behavior, and biological activity of bisazomethine dye derived from 2,3-diaminomaleonitrile and 2-hydroxy-1-naphthaldehyde and its zinc complex

Elham S. Aazam [a], Mohamed M. Ghoneim [b] & Mona A. El-Attar [b]
[a] Department of Chemistry, Girls Campus, University of King Abdulaziz, P.O. Box 6171, Jeddah 21442, Saudi Arabia
[b] Analytical Chemistry Research Unit, Chemistry Department, Faculty of Science, Tanta University, 31527-Tanta, Egypt
Published online: 18 Jul 2011.

To cite this article: Elham S. Aazam, Mohamed M. Ghoneim & Mona A. El-Attar (2011) Synthesis, characterization, electrochemical behavior, and biological activity of bisazomethine dye derived from 2,3-diaminomaleonitrile and 2-hydroxy-1-naphthaldehyde and its zinc complex, Journal of Coordination Chemistry, 64:14, 2506-2520, DOI: 10.1080/00958972.2011.600453

To link to this article: http://dx.doi.org/10.1080/00958972.2011.600453

Journal of Coordination Chemistry
Vol. 64, No. 14, 20 July 2011, 2506–2520

Synthesis, characterization, electrochemical behavior, and biological activity of bisazomethine dye derived from 2,3-diaminomaleonitrile and 2-hydroxy-1-naphthaldehyde and its zinc complex

ELHAM S. AAZAM*†, MOHAMED M. GHONEIM‡ and MONA A. EL-ATTAR‡

†Department of Chemistry, Girls Campus, University of King Abdulaziz, P.O. Box 6171, Jeddah 21442, Saudi Arabia
‡Analytical Chemistry Research Unit, Chemistry Department, Faculty of Science, Tanta University, 31527-Tanta, Egypt

(*Received 21 March 2011; in final form 6 June 2011*)

Bisazomethine containing diaminomaleonitrile, (bhnmab) and its Zn-complex were synthesized by both classical and microwave-assisted methods and characterized by ^{1}H-NMR, ^{13}C-NMR, UV-Vis, FT-IR, DSC, TG, fluorescence, and cyclic voltammetry. The solvatochromic responses of bhnmab in solvents of different polarities exhibited positive solvatochromism with a large bathochromic shift from benzene to DMF. The emission of [Zn(II)-(bhnmab)(sol)] is red-shifted and much more intense when compared with that of bhnmab. A square-pyramidal structure for the formed complex has been proposed using a CS Chem 3D Ultra Molecular Modeling and Analysis Program. The electrochemical behavior of bhnmab and its Zn(II) complex in B–R universal buffer containing 30% (v/v) of DMF was examined by cyclic voltammetry. *In vitro* antimicrobial activity of various concentrations of bhnmab and its Zn(II) complex were assessed using the cup plate diffusion method. The Zn(II) complex exhibited higher antimicrobial activity than the free ligand ($p \leq 0.05$).

Keywords: Schiff base 2,3-Diaminomaleonitrile; Zn(II) complex; Solvatochromism; Voltammetry; Biological activity

1. Introduction

Transition-metal complexes with Schiff-base ligands are promising materials for optoelectronic applications due to their outstanding photoluminescent (PL) and electroluminescent (EL) properties; the ease of synthesis readily allows structural modification for optimizing of material properties. Zn(II)-Schiff base polymers formed by self-assembly reactions of Zn(II) salts and salicylaldimine monomers exhibited blue to yellow PL. Polymer light-emitting devices (PLEDs) employing these polymers as emitters give green or orange EL [1]. Bis-azomethine dyes derived from 2,3-diaminomaleonitrile with arylaldehydes are reported as extremely bright [2, 3], tinctorially strong disperse dyes useful for dying and printing polyester and

*Corresponding author. Email: wayfield8@yahoo.com

ISSN 0095-8972 print/ISSN 1029-0389 online © 2011 Taylor & Francis
DOI: 10.1080/00958972.2011.600453

polyester–cotton blend fibers in yellow to blue shades. Recently, these dyes were examined as red light-emitting materials in organic EL devices [4, 5]. Solvatochromic D–π–A charge transfer dyes attract much attention because of their applicability as probes for the determination of solvent polarity as well as their potential application as colorimetric chemo-sensors for volatile organic compounds [6–8]. Charge transfer dyes have also been developed for using PL and EL materials in dye laser sensors and optical light-emitting diodes (OLEDs). Solvatochromism involves a change in the absorption or emission spectra when dissolved in solvents with different polarities [9].

Microwave (MW) irradiation can accelerate chemical processes, particularly reducing the reaction time and energy input in reactions run for a long time at high temperatures under conventional conditions [10–12]. Electrochemical behavior of Schiff-base complexes in various supporting electrolytes was discussed [13–16]. Schiff bases and most of their metal complexes display inhibitor effects against different microorganisms [17–22]. Zinc is the second most abundant transition-metal ion in the human body, playing crucial roles in many important biological processes acting as structural and catalytic cofactors [23]. It has also been used to probe the role of the metal center in second-order nonlinear optical properties [24].

In this study we report the synthesis of a bisazomethine Schiff base containing diaminomaleonitrile (bhnmab) and its Zn(II) complex, applying MW irradiation for the synthesis in order to check whether such activation might influence yield, selectivity, and time of reaction in comparison with a conventional thermal treatment under similar conditions. The choice of Zn(II) as the metal center was guided by previous observations of enhanced fluorescence upon Zn(II)-complex formation [25, 26]. 3-D molecular modeling of the proposed structure of the investigated compounds was also studied using a CS Chem 3D Ultra Molecular Modeling and Analysis Program [27]. Antibacterial activities of bhnmab and its Zn(II) complex are discussed.

2. Experimental

2.1. *Materials and solutions*

(a) The reagents used in this study were diaminomaleonitrile and 2-hydroxy-1-naphthaldehyde (Aldrich), zinc(II) acetate dehydrate (BDH), tetrahydrofuran (THF), dichloromethane (DCM), dimethylformamide (DMF), ethyl acetate (EtOAc), acetonitrile (MeCN), dimethyl sulfoxide (DMSO), methanol (MeOH), isopropanol (IPA), benzene, chloroform (TCM), ethanol (EtOH), and PET (petroleum ether 60–80°C) (BDH). For HPLC analysis, MeCN and EtOAc were HPLC grade.

(b) Standard stock solutions (2.5×10^{-3} mol L^{-1}) of bhnmab and its Zn(II) complex were obtained by dissolving solid compound in appropriate volume of DMF. More dilute solutions ($1 \times 10^{-3} \times 10^{-4}$ mol L^{-1}) were prepared by accurate dilution of the standard stock solution with DMF.

(c) A series of Britton–Robinson (B–R) universal buffer of pH 2–11 was prepared in twice-distilled water [28] and used as a supporting electrolyte in the presence of 30% (v/v) of DMF.

(d) The different strains of both pathogenic Gram-positive bacteria (G^+) {*Bacillus subtilis*, *Staphylococcus epidermidis*, *Micrococcus luteus*, *Staphylococcus aureus*, and *Bacillus cereus*} and Gram-negative bacteria (G^-) {*Klebsiella pneumoniae*, *Shegella dysenteriae*, *Aeromonas hydrophila*, *Escherichia coli*, and *Serratia marcescens*} were used for testing the biological activity of various concentrations of bhnmab and its Zn-complex (2.5×10^{-3}, 1×10^{-3}, and 1×10^{-4} mol L^{-1}) in DMF. The various organisms used in this study were provided by the Microbiology Laboratory, Faculty of Science, Tanta University, Egypt. The organisms were confirmed by biochemical tests. Both commercial Erythrocin tablets {Erythromycin, (G^+)} and Amikin vial {Amikacin sulfate, (G^-)} were used as standard antibacterial agents for comparison with bhnmab and its Zn-complex.

(e) Nutrient agar solid medium contained per 1000 mL (pH = 7.2): beef extract 3 g, peptone 5 g, nail 5 g, and agar 20 g (Merck) was used for growing the tested microorganisms.

2.2. *Apparatus and procedures*

2.2.1. Physical measurements. Elemental analysis was determined in the Micro Analytical Unit using Perkin Elmer 2400 (London, Metropolitan University, UK). Infrared (IR) spectra of solids were recorded on a Perkin Elmer 100 FT-IR spectrophotometer. UV-Vis spectra were recorded on a Varian 2300 spectrophotometer. ^{1}H and ^{13}C-NMR spectra were recorded on a Varian 400 MHz spectrometer and a Varian 500 MHz spectrometer. The ^{1}H and ^{13}C-NMR chemical shifts (δ, ppm) are given relative to residual solvent peaks. The fluorescence spectra of the compounds in different solvents were recorded on a FW WINLAB LS-45 Fluorescence Spectrophotometer (Perkin Elmer). TG and DTA analyses were carried out under air and nitrogen with a heating rate of 20°C min^{-1} using a Perkin Elmer TGA 47 analyzer. DSC analysis was carried out using a Perkin Elmer DSC pyris1. MW oven was used in all synthesis (430 W). Melting points were measured using a melting point apparatus (Gallenkamp, UK). HPLC analyses were performed on a C_{18} (YMC-Pack ODS-AQ) column (5 µm, 4.6 mm × 250 mm) using a Perkin Elmer Series 200B HPLC system consisting of a UV/VIS detector at 254 nm with MeCN–EtOAc as eluent (20 : 80 v/v). The flow rate of the mobile phases was 1.0 mL min^{-1} and the column temperature was 90°C.

2.2.2. Electrochemical measurements. A computer-controlled Potentiostat/Galvanostat Model 273A-PAR and the electrode assembly model 303A (Princeton Applied Research, Oak Ridge, TN, USA) with the software package 270/250-PAR were used in cyclic voltammetric measurements. A micro-electrochemical cell with three-electrode system comprised a hanging mercury drop electrode (HMDE) as a working electrode (surface area = 0.026 cm^2), an Ag/AgCl/KCl reference electrode and a platinum wire auxiliary electrode were used. A pH-meter Model HI8014 (Hanna Instruments, Italy) accurate to ±0.01 pH units was used for pH measurements. AquaMatic bi-distillation water system (Hamilton Laboratory Glass Ltd., Kent, UK) was used to obtain de-ionized water. A Mettler balance (Toledo-AB104, Switzerland) was used for weighing the solid materials.

A solution (1×10^{-3} mol L^{-1}) of the examined compounds in 10 mL B–R universal buffer containing 30% (v/v) of DMF was introduced into the electrochemical cell, and then deoxygenated with pure nitrogen gas for about 10 min in the first cycle measurements and for 30 s in each successive one, while a stream of nitrogen gas was kept over the solution during the measurements.

2.2.3. Biological activity. The antimicrobial tests were performed by the cup plate diffusion method [29, 30]. The test organisms were grown on nutrient agar medium in petri plates. It was allowed to soak for 15 min and then boiled in a water bath until the agar was completely dissolved. The mixture was autoclaved at 120°C for 30 min, poured into previously washed and sterilized petri plates (dry heat in an oven at 160°C for 2 h), and allowed to solidify at room temperature. All the petri plates were aseptically flooded with 0.1 mL of prepared bacterial suspension which was evenly spread. Wells of 10 mm were bored aseptically using a sterile cork borer. The agar plugs were taken out carefully to avoid disturbing the surrounding medium. The wells were filled completely with tested solution (0.05 mL of 2.5×10^{-3}, 1×10^{-3}, or 1×10^{-4} mol L^{-1}) using sterile microliter-pipette, and then the plates were kept in an incubator at 37°C for 18 h to activate the bacterial strain. After incubation the petri plates were observed for antibacterial activity and the diameters of inhibition zones (the clear zones around the holes killing the bacteria) were measured by a fine ruler in millimeters [31]. The experiments were repeated in triplicate under similar conditions to check the reproducibility of the results and the mean value obtained was used to calculate the zone of growth inhibition of each sample.

Erythrocin tablets (Kahira Pharm. & Chem. Ind. Co., Egypt under License of Abbott Laboratories) with declared content of 250 mg erythromycin/tablet was used as a standard for Gram-positive bacteria. The content of five tablets was weighed. Then, they were grounded to a homogeneous fine powder. A weighed portion of the homogeneous powder equivalent to 500 mg of erythrocin was transferred accurately into a 100 mL-volume calibrated flask containing 70 mL DMF. Then, the contents were sonicated for 15 min and the volume was completed to the mark with DMF. More diluted solutions of Erythrocin tablets (2.5×10^{-3}, 1×10^{-3}, and 1×10^{-4} mol L^{-1}) were obtained by accurate dilution of the prepared solution with DMF. Amikin (amikacin sulfate in 2 mL aqueous solution; Smithkline Beecham, Egypt LLC) was used as a standard for Gram-negative bacteria. The desired concentrations of Amikin (2.5×10^{-3}, 1×10^{-3}, and 1×10^{-4} mol L^{-1}) were prepared by accurate dilution of the solution with de-ionized water. DMF was used as a negative control.

2.2.4. Statistical analysis. Statistical analysis of antimicrobial activity of various concentrations (2.5×10^{-3}, 1×10^{-3}, and 1×10^{-4} mol L^{-1}) of the synthesized compounds as well as the standard drugs was performed using SPSS 1601EW program to determine the degree of significance between treatments using two-way analysis of variance (ANOVA) at $p \leq 0.05$. Results were presented as mean ± standard deviation (SD). All the data were statistically analyzed by the methods described by Cochran *et al.* [32].

2.2.5. Molecular modeling and analysis. As we were unable to prepare crystals of the prepared compounds suitable for X-ray diffraction, the obtained molecular modeling for the investigated compounds was analyzed using a CS Chem 3D Ultra Molecular Modeling and Analysis Program [27]. This allows obtaining of a rapid structure building, geometry optimization with minimum energy, and molecular display.

2.3. *Synthesis of the investigated bis-Schiff base and its Zn-complex*

2.3.1. Preparation of 2,3-bis[(2-hydroxynaphthalen-1-yl)methyldiene]amino-but-2-enedinitrile (bhnmab) by solvothermal method (Method A). 2,3-Diaminomaleonitrile (0.16 g, 1.45 mmol) in 15 mL of ethanol was added to a stirred solution of 2-hydroxy-1-naphthaldehyde (0.5 g, 2.9 mmol) in 25 mL of absolute ethanol. The mixture turned red-brown immediately and was refluxed overnight then cooled to room temperature and a brown precipitate formed. The product was collected by filtration as a brown solid. Recrystallization from chloroform by slow evaporation afforded orange needles. The purity of the product was estimated by TLC {EtOAc-PET (2 : 8 V/V)} and NMR spectroscopy. Yield (66.7%, 0.4 g, 0.96 mmol), m.p. (248°C). UV-Vis: λ_{max} nm $(10^{-5}\,(\text{mol L}^{-1})^{-1}\,\text{cm}^{-1})$ (THF): 250, 350, 384, 460 and 595 nm. ^{1}H-NMR (DMSO-d_6, 500 MHz): δ (ppm) = 7.00(d, J = 9.0 Hz, 2H), 7.43(t, J = 7.4 Hz, 2H), 7.62(t, J = 7.6 Hz, 2H), 7.91–7.81(m, 2H), 8.0(d, J = 8.9 Hz, 2H), 8.63(d, J = 8 Hz, 2 H), 9.26(s, 2H, N=CH), and 11.94(s, 2H, OH). ^{13}C-NMR (DMSO-d_6, 400 MHz): δ (ppm) = 103.88, 110.24, 114.04, 114.61, 118.46, 121.94, 123.88, 125.10, 127.85, 128.54, 128.89, 131.66, 131.66, 131.66, 13.20, 154.88, and 159.74. Anal. Calcd for $C_{26}H_{18}N_4O_3$ [bhnmab + H_2O]: C, 71.88; H, 4.18; N, 12.90. Found (%): C, 72.20; H, 4.10; N, 12.97. EI-MS: m/z 416, 17% $[\text{bhnmab}]^+$.

2.3.2. Preparation of 2,3-bis[(2-hydroxynaphthalen-1-yl)methyldiene]amino-but-2-enedinitrile (bhnmab) by MW-assisted method (Method B). 2,3-Diaminomaleonitrile (0.6 g, 5.56 mmol), 2-hydroxy-1-naphthaldehyde (1.92 g, 11.12 mmol), and 80 mL of ethanol were mixed in a conical flask capped with a glass cover and placed in a MW oven (430 W) and irradiated for 5 min. The product was cooled to room temperature and washed with 2 mL of ethanol. The purity of the resultant brown solid was estimated by TLC {EtOAc-PTE (2 : 8 v/v)} and NMR spectroscopy. Yield (78%, 1.8 g, 4.33 mmol), m.p. (248°C). The chemical reaction for synthesis of bhnmab is shown in scheme 1.

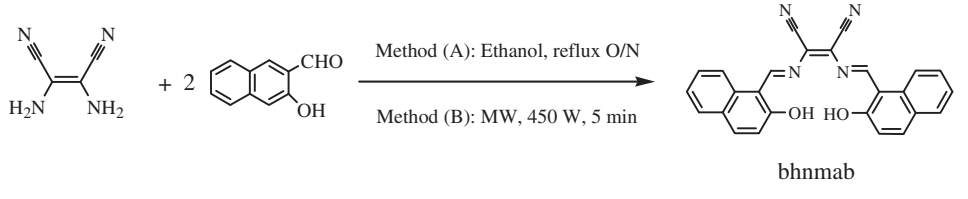

bhnmab

Scheme 1. Synthesis of bhnmab.

2.3.3. Preparation of 2,3-bis[(2-hydroxynaphthalen-1-yl)methyldieneamino-but-2-enedinitrile zinc [Zn(II)-bhnmab(sol)] by solvothermal method (Method A). Zinc acetate dihydrate (0.053 g, 0.24 mmol) in 10 mL of ethanol was added to a stirred solution (0.1 g, 0.24 mmol) of 2,3-bis(2-hydroxynaphthalen-1-yl)methyldiene)amino)but-2-enedinitrile (bhnmab) in 20 mL of ethanol. The mixture was refluxed overnight then cooled to room temperature, upon which a black-violet precipitate formed. The product was collected by filtration and washed with 2 mL of ethanol, and then air dried. Yield (63.6%, 0.07 g, 0.14 mmol), m.p. decom >360°C. ^{1}H-NMR (DMSO-d_6, 400 MHz): δ (ppm) = 3.3(s, DMSO-d_6 + H_2O, s), 7.0(d, J = 9.3 Hz, 2H), 7.33(t, J = 7.4 Hz, 2H), 7.57(t, J = 7.3 Hz, 2H), 7.76(d, J = 7.4 Hz, 2H), 7.93(d, J = 9.3 Hz, 2H), 8.1(d, J = 8.6 Hz, 2H) and 9.32(s, 2H, N=CH). ^{13}C-NMR (DMSO-d_6, 400 MHz): δ (ppm) = 18.69(CH_3CH_2OH), 56.16(CH_3CH_2OH), 109.72, 112.28, 119.38, 121.09, 123.50, 126.27, 127.14, 129.36, 134.87, 139.14, 155.68, and 176.85. Anal. Calcd for $C_{26}H_{16}N_4O_3Zn$ [Zn-bhnmab(H_2O)]: C, 62.73; H, 3.24; N, 11.25. Found (%): C, 62.81; H, 3.19; N, 11.18. EI-MS: m/z 478 (40%), 480 (34%), 482 (23%) [Zn-bhnmab]$^+$.

2.3.4. Preparation of 2,3-bis[(2-hydroxynaphthalen-1-yl)methyldiene]amino-but-2-enedinitrile zinc [Zn(II)-bhnmab(sol)] by MW-assisted method (Method B). Zinc acetate dihydrate (0.053 g, 0.24 mmol) was added to a solution (0.1 g, 0.24 mmol) of 2,3-bis(2-hydroxynaphthalen-1-yl)methyldiene)amino)but-2-enedinitrile (bhnmab) in 10 mL of ethanol. The mixture was placed in a conical flask capped with a glass cover and placed in a MW oven (430 W) and irradiated for 1 min. The product was cooled to room temperature, filtered, and washed with 2 mL of ethanol. The purity of the resultant blue-black solid was confirmed by HPLC analysis on a C_{18} column with acetonitrile–methyl acetate (20 : 80 v/v) mobile phase at a retention time of 3.11 min. Only one absorption band for the zinc complex appeared. The obtained yield is 90%, 0.1 g, 0.21 mmol; m.p. decom. >360°C.

2.3.5. Preparation of 2,3-bis[(2-hydroxynaphthalen-1-yl)methyldiene]amino-but-2-enedinitrile zinc [Zn(II)-bhnmab(sol)] by MW-template reaction method (Method C). 2,3-Diaminomaleonitrile (0.06 g, 0.58 mmol), 2-hydroxy-1-naphthaldehyde (0.2 g, 1.16 mmol), zinc acetate dihydrate (0.13 g, 0.58 mmol), and 20 mL of ethanol were mixed in a conical flask capped with a glass cover and placed in a MW oven (430 W) and irradiated for 1 min. The product was cooled to room temperature, filtered, and washed with 2 mL of ethanol. The purity of the product was checked by NMR spectroscopy. Yield (93%, 0.27 gm, 0.13 mmol), m.p. decom. >360°C. The chemical reaction for synthesis of [Zn-(bhnmab)(sol)] is shown in scheme 2.

3. Results and discussion

3.1. *Physico-chemical characterizations*

Condensation of 2,3-diaminomaleonitrile in ethanol with 2-hydroxy-1-naphthaldehyde proceeded in the absence of a base in a ratio of 1 : 2 to give the symmetrical

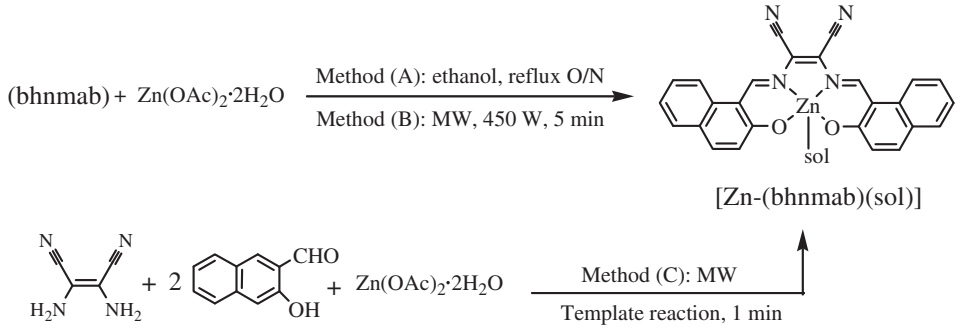

Scheme 2. Synthesis of [Zn(II)-(bhnmab)(sol)].

bis-azomethine dye (bhnmab), which was confirmed by ^{1}H-NMR spectroscopy (scheme 1). As shown in scheme 2, the formation of [Zn(II)-bhnmab(sol)] occurred by refluxing bhnmab with zinc acetate dihydrate in a 1 : 1 molar ratio in ethanol (Method A) or *via* MW-assisted reaction of bhnmab with zinc acetate dihydrate in a 1 : 1 molar ratio in ethanol (Method B) or *via* template-MW-assisted synthesis (Method C). The yield of bhnmab was 66.7% (Method A) and 78% (Method B), while for [Zn(II)-bhnmab] the yields were 63.6%, 90%, and 93% (Methods A, B, and C, respectively). The higher yields with less reaction time make MW methods (B and C) superior to the solvothermal method. bhnmab and its Zn(II) complex are stable at room temperature; bhnmab is soluble in common polar organic solvents, such as EtOH, MeCN, DMSO, and DMF, but partially soluble in benzene. The prepared Zn(II) complex is highly soluble in DMF, DMSO, MeCN, DCM, and THF, but moderately soluble in EtOH, MeOH, IPA, and EtOAc. bhnmab and its Zn(II) complex were characterized by elemental analysis, spectral, NMR, and electrochemical measurements. The geometry of the newly synthesized compounds has been elucidated based on their elemental analysis, NMR, TG, DTG, spectral data, and molecular modeling study.

3.2. *IR spectrum*

The IR spectrum of bhnmab showed that the medium absorption band at 3468 cm^{-1} is due to ν(OH). The medium intensity band at 3337 cm^{-1} may be due to intermolecular OH–OH hydrogen bonds. Bands at 3192–2922 cm^{-1} are due to asymmetric and symmetric stretching vibrations of aromatic CH groups. For [Zn(II)-bhnmab(sol)] a broad variable band at 3981 cm^{-1} is attributed to OH of the coordinated water or ethanol molecule. The shift of νC=N from 1599 cm^{-1} in bhnmab to 1567 cm^{-1} in [Zn(II)-bhnmab(sol)] indicated the formation of the designed complex with bis-azomethine nitrogen coordination. The IR spectrum of bhnmab may be easily fingerprinted by two sharp –C≡N bands at 2240 and 2204 cm^{-1} due to b_1 and b_{2u}; however, only one sharp band was observed for its Zn(II) complex at 2207 cm^{-1} [33], indicating that Zn(II) modifies the electronic structure [24].

3.3. *Thermal analysis*

DSC thermograms of bhnmab and [Zn(II)-bhnmab(sol)] were recorded under nitrogen with a heating rate of $10^{\circ}C\,min^{-1}$. bhnmab has a small peak at 220–250°C indicating its melting, while the Zn(II) complex undergoes some phase changes at 320–375°C. The small exothermic peak at 320°C may be due to phase change and the small endothermic peak at 375°C may be due to the loss of coordinated solvent. The TG and DTG curves of bhnmab and [Zn(II)-bhnmab(EtOH)] in nitrogen were recorded at a heating rate of $20^{\circ}C\,min^{-1}$ from 40°C to 800°C (Supplementary material). The initial weight loss in bhnmab is due to the loss of water of crystallization. The thermal decomposition of [Zn(II)-bhnmab(EtOH)] took place in two steps as indicated by DTG peaks at 150–250°C and 385–460°C. Weight loss in the first step is 9% (8.8%, theoretically calculated for loss of one ethanol). The Zn(II) complex remains stable to 385°C and the second step weight loss is 78%, which coincides with 79.2%, theoretically calculated for loss of bhnmab. The TG curve showed 87% total mass loss at 460°C (88% theoretical value), indicating complete removal of bhnmab and ethanol. The main residual product was Zn metal at 500–800°C with 13% (theoretical 12%). Thus, thermal analysis indicated higher stability of the Zn(II) complex over bhnmab [34].

3.4. *Structure of the synthesized compounds*

Formation of bhnmab was evidenced by the disappearance of CHO in the ^{1}H-NMR at $\delta = 13.13$ ppm and shift of phenolic OH to higher field $\delta = 11.94$ ppm. The azomethine protons appeared as a singlet at 9.26 ppm. Multiple signals observed at 8.63–7.23 ppm are due to naphthalene aromatic protons. EI-MS data are consistent with the formation of bhnmab, while elemental analysis, TG, DTG, and NMR data support the presence of water of crystallization.

Formation of [Zn(II)-bhnmab(EtOH)] was inferred from disappearance of phenolic OH in the ^{1}H-NMR spectrum. EI-MS data are consistent with the formation of [Zn(II)-bhnmab], showing the most important three fragments at m/z 478, 480, and 482 corresponding to the three important isotopes of zinc 64, 66, and 68, respectively, with the correct isotopic distribution. NMR data are consistent with the expected structure, also indicating the presence of coordinated ethanol (as supported by TG and DTG data). The azomethine protons shifted to lower field at 9.32 ppm than the free ligand. The aromatic protons appeared as multiplets at 8.11–6.99 ppm. In comparison to the ^{13}C-NMR spectrum of the free ligand, azomethine carbons were greatly affected upon coordination to zinc shifting from 159.74 to 176.85 ppm. [Zn(II)-bhnmab(EtOH)] likely has a square-pyramidal arrangement with an apical ethanol or water as indicated by elemental analysis, as observed in several related structures [24].

3.5. *Molecular modeling studies*

In Zn(II)-bhnmab complex, zinc coordinates to bhnmab through two nitrogens of azomethine and two phenolate oxygens (figure 1). Values of the bond angles (°) between O–Zn–N, O–Zn–O and N–Zn–N range from 41.3745 to 157.2754. The calculations show that Zn–N length (Å) is longer than Zn–O. The bond angles (°) of azomethine–nitrogen in bhnmab are affected by complexation to zinc, where the C=N bond length

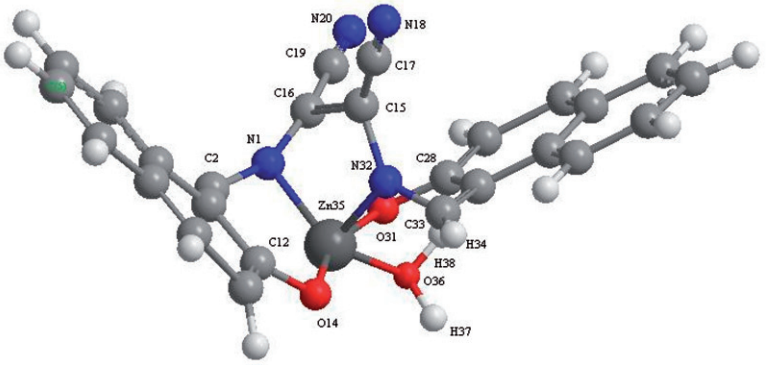

Figure 1. Geometry optimized structure of [Zn-bhnmab(H_2O)].

Table 1. Data of absorption spectra and $E_T(30)$ values of bhnmab in various solvents.

Solvent	λ_{max} (nm)	$E_T(30)$ (kcal mol^{-1})
Benzene	534.98	34.3
Chloroform (TCM)	539.95	39.1
Dichloromethane (DCM)	545.06	40.7
Dimethylformamide (DMF)	619.94	43.8
Dimethylsulfoxide (DMSO)	525.03	45.1
Acetonitrile (MeCN)	520.05	45.6
Ethanol (EtOH)	599.98	51.9

is longer in the Zn(II) complex compared to the free ligand. Selected calculated bond lengths and angles obtained from *ab initio* calculations for bhnmab and its Zn(II) complex are given in Supplementary material [27]. Molecular modeling showed that the Zn(II)-bhnmab complex has a square-pyramidal structure completed by coordination of a water molecule (figure 1). For the different bond lengths (Å) and angles (°), the various atoms are numbered in Arabic numerals.

3.6. *Electronic spectra*

As shown in table 1, bis-azomethine dye (bhnmab) exhibited strong solvatochromic properties in solvents with different polarities (benzene, TCM, DCM, DMF, DMSO, MeCN, and EtOH) (Supplementary material).

As the solvent polarity increased going from benzene to DMF, a bathochromic shift was observed (i.e. positive solvatochromism) accompanied by a change in color from orange to green (Supplementary material).

The dependence of the absorption maximum on $E_T(30)$ solvent polarity parameter can be fitted to almost linear function showing selective stabilization of the ground state for DMF; however, above an $E_T(30)$ value of 43.8 kcal mol^{-1} no significant solvent-polarity-dependent spectral shifts in the absorption spectrum were observed (table 1). This indicates that the chromophore in its ground state is not significantly stabilized by

coordination of solvent [8]. Other factors such as changes in the hydrogen-bonding strength and/or due to excited state protonation may affect the solvatochromic behavior [6]. Very large ε_{max} values over 100,000 indicated that the absorption is due to intramolecular charge transfer (ICT) of the chromophoric system in which naphthalene is a donor and central ethylene is an acceptor [5]. The ε_{max} for [Zn(II)-(bhnmab)(sol)] = 1.71×10^5 L mol^{-1} cm^{-1}.

Compared to bhnmab the absorption maximum for its Zn(II) complex was blue shifted in DMF, with high intensity (figure 2; spectra 1 and 2). The Zn(II) complex exhibited remarkable red emission when compared to bhnmab under illumination (Supplementary material).

Slight solvatochromic effect was observed for [Zn(II)-bhnmab(sol)] in THF, DCM, DMF, EtOAc, MeCN, DMSO, MeOH, IPA, and EtOH, indicating that the tautomerism involving keto/enol structures of bhnmab has stopped upon complexation. Similar variable peak shapes were observed for the complex in the various solvents and the peak positions were very close, having absorption maxima between 587 and 604 nm (Supplementary material).

The fluorescence of bhnmab and its Zn(II) complex were measured in MeCN at an absorbance value <0.1 at room temperature. As shown in figure 3, fluorescence emission spectra for bhnmab and its Zn(II) complex exhibited strong emission peaks at 556 (figure 3; spectrum 1) and 625 nm (figure 3; spectrum 2), respectively, when excited

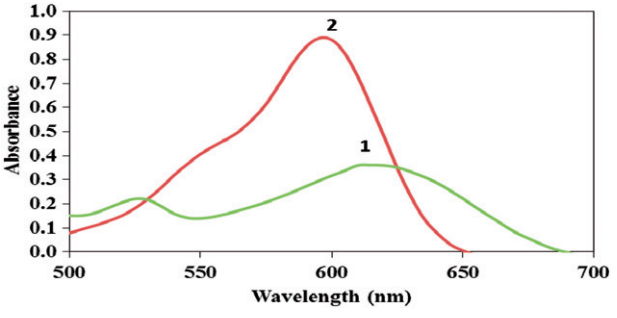

Figure 2. The UV-Vis absorption spectra of 1.2×10^{-5} mol L^{-1} of bhnmab (**1**) and its Zn complex (**2**) in DMF.

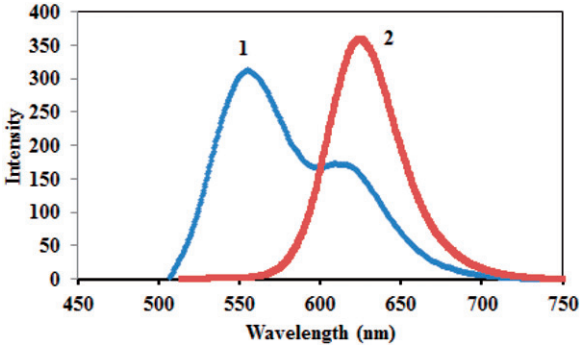

Figure 3. The emission spectra of bhnmab (**1**) and its Zn complex (**2**) in MeCN at an excitation wavelength of 496 nm.

at 496 nm. The peak of the Zn(II) complex was higher in intensity and red shifted when compared to that of bhnmab, and the quantum yield of the Zn(II) complex is 15 times higher than that of bhnmab. Enhancement of fluorescence and the significant red shift of [Zn(II)-bhnmab(sol)] compared to bhnmab were attributed to introduction of Zn^{2+}, which imposes rigidity and hence decreases the non-radiative decay of the excited states [35].

3.7. *Electrochemical studies*

Cyclic voltammograms of 1×10^{-4} mol L^{-1} bhnmab in B-R universal buffer of pH ≤ 8 containing 30% (v/v) DMF at different sweep rates (100–500 mV s^{-1}) exhibited a single irreversible cathodic peak, which may be attributed to reduction of C=N double bonds (figure 4). The peak current (i_p) decreased upon increase in pH until vanishing at pH >8, indicating that the limiting current is controlled by the rate of protonation [36–38]. No anodic peak was observed on the reverse sweep, confirming the irreversible nature of the electrode reaction (figure 4). The peak potential (E_p) shifted to more negative values upon increase in pH (figure 4; inset), indicating involvement of protons in the electrode reaction and that the proton-transfer reaction precedes the electron transfer [39]. The E_p (V) *versus* pH plot over pH range 2.4–8.8 was a broken line with intersection at pH 6.2 (figure 4; inset), which may correspond to an acid–base equilibrium (pK_a) in bhnmab. A linear relationship of the peak potential E_p (V) *versus* pH of the medium (2.4–5.5) at scan rate (v) of 500 mV s^{-1}, following the regression equation E_p (V) $= 0.073$ pH $+ 0.78$ ($r = 0.997$ and $n = 4$), was obtained. From its slope

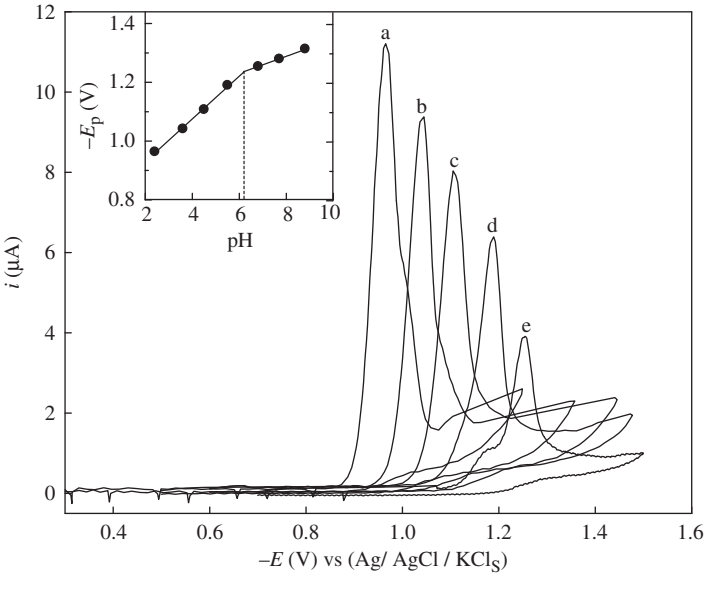

Figure 4. Cyclic voltammograms of 1×10^{-4} mol L^{-1} of bhnmab at scan rate of 500 mV s^{-1} in B–R universal buffer of various pH values containing 30% (v/v) DMF: (a) 2.4, (b) 3.6, (c) 4.5, (d) 5.5, and (e) 6.8. Inset: E_p *vs.* pH for bhnmab.

$(0.059/\alpha n_a)$, the value of αn_a was estimated (0.82), and consequently value of the symmetry transfer coefficient α was found to be 0.41 at $n_a = 2$.

The peak potential E_p shifted to more negative values with increase in scan rate (100–500 mV s^{-1}), providing additional support of the irreversible nature of the electrode processes [40]. From the slope values (15–20 mV) of the obtained linear plots of E_p *versus* ln$v$ (slope, mV $= 12.85/\alpha n_a$) [41] values of αn_a (0.64–0.86) and α (0.32–0.43) were estimated at $n_a = 2$, confirming again the irreversible nature of the electrode processes of the examined compound [40, 42].

Cyclic voltammograms of [Zn(II)-(bhnmab)(sol)] were also recorded under the same experimental conditions at different sweep rates (100–500 mV s^{-1}) and were found to exhibit one quasi-reversible redox couple over the entire pH ranges (3.6–5.5), assumed to be reduction of Zn(II) to Zn(I) (Supplementary material), besides an irreversible cathodic peak at more negative potential corresponding to reduction of the C=N double bonds of bhnmab as for the free ligand (figure 4). The difference in peak separation ($\Delta E_p = E_p^c - E_p^c = 0.059/n$ V) varies from 0.04 to 0.24 V and increases with increasing scan rate. The anodic to cathodic peak current ratio (i_p^a/i_p^c) equals unity, dependent on sweep rate used. The current function ($i_p/v^{1/2}$) depends on the scan rate. These data are compatible with a quasi-reversible electrode reaction.

3.8. *Biological activity*

The *in vitro* biological activities of bhnmab and its Zn(II) complex were tested against 10 strains of pathogenic Gram-positive and Gram-negative bacteria using the cup plate diffusion method [29, 30] in DMF. Erythrocin tablets and Amikin vial as standard antibacterial agents and pure DMF were tested for their antibacterial activities at the same concentrations and conditions. The standard drugs exhibited high biological activity against the studied strains of bacteria (table 2), although Erythrocin tablets showed no antibacterial activity against *S. epidermidis* (table 2). DMF showed no activity against any microbial strains (Supplementary material). bhnmab and its Zn(II) complex exhibit varying inhibitory effects on the growth of the tested bacterial species when compared with the standard drugs (table 2).

The mean value obtained for three individual replicates of inhibition zones (table 2) of bhnmab showed biological activity against *S. aureus* (G^+) and *E. coli* (G^-) at various concentrations (2.5×10^{-3}, 1×10^{-3}, and 1×10^{-4} mol L^{-1}), however, against *B. subtilis* (G^+) only at high concentration (2.5×10^{-3} mol L^{-1}) and no biological activity toward *S. epidermidis* (G^+), *M. luteus* (G^+), *B. cereus* (G^+), *K. pneumoniae* (G^-), *S. dysenteriae* (G^-), *A. hydrophila* (G^-), and *S. marcescens* (G^-) (Supplementary material). Most of the investigated pathogenic bacterial strains were resistant to bhnmab.

[Zn(II)-(bhnmab)(sol)] exhibited biological activities against *S. aureus* (G^+), *B. cereus* (G^+), *K. pneumoniae* (G^-), *S. dysenteriae* (G^-), *A. hydrophila* (G^-), *E. coli* (G^-), and *S. marcescens* (G^-) at various concentrations (2.5×10^{-3}, 1×10^{-3}, and 1×10^{-4} mol L^{-1}) (table 2) and has activity against *B. subtilis* (G^+), *S. epidermitdis* (G^+), and *M. luteus* (G^+) only at high concentration (2.5×10^{-3} mol L^{-1}) (table 2), (Supplementary material). *S. epidermidis* (G^+) showed complete resistance to both ligand and the standard Erythrocin tablets, whereas it has a high sensitivity to the Zn(II) complex (table 2).

Table 2. Diameters (mm) of growth inhibition zones of various concentrations of synthesized compounds and standard drugs against selected bacterial strains in DMF using the cup plate diffusion method.

		Zone of inhibition (mm) (Mean ± SD)			
Organisms	Conc. (mol L^{-1})	Erythrocin (tablets)	Amikin (vial)	bhnmab	Zn-bhnmab
B. Subtilis (G^+)	2.5×10^{-3}	25.0 ± 0.2		14.4 ± 0.6	19.4 ± 0.6
	1.0×10^{-3}	23.1 ± 0.5		–	–
	1.0×10^{-4}	15.0 ± 0.4		–	–
S. epidermidis (G^+)	2.5×10^{-3}	–		–	19.3 ± 0.9
	1.0×10^{-3}	–		–	–
	1.0×10^{-4}	–		–	–
M. luteus (G^+)	2.5×10^{-3}	34.6 ± 0.6		–	14.8 ± 0.2
	1.0×10^{-3}	32.0 ± 0.6		–	–
	1.0×10^{-4}	30.0 ± 0.6		–	–
S. aureus (G^+)	2.5×10^{-3}	25.0 ± 0.1		9.5 ± 0.5	14.4 ± 0.5
	1.0×10^{-3}	23.0 ± 0.2		7.8 ± 0.2	9.3 ± 0.7
	1.0×10^{-4}	18.0 ± 0.2		4.6 ± 0.3	7.6 ± 0.3
B. cereus (G^+)	2.5×10^{-3}	32.0 ± 0.5		–	9.5 ± 0.5
	1.0×10^{-3}	30.0 ± 0.8		–	6.8 ± 0.2
	1.0×10^{-4}	25.0 ± 0.5		–	4.9 ± 0.6
K. pneumonia (G^-)	2.5×10^{-3}		30.0 ± 0.7	–	19.2 ± 0.7
	1.0×10^{-3}		26.0 ± 0.3	–	15.4 ± 0.6
	1.0×10^{-4}		20.0 ± 0.7	–	12.6 ± 0.4
S. dysenteriae (G^-)	2.5×10^{-3}		33.0 ± 0.3	–	19.4 ± 0.8
	1.0×10^{-3}		30.0 ± 0.8	–	11.9 ± 0.1
	1.0×10^{-4}		20.0 ± 0.5	–	7.8 ± 0.2
A. hydrophila (G^-)	2.5×10^{-3}		33.0 ± 0.7	–	17.4 ± 0.5
	1.0×10^{-3}		32.0 ± 0.7	–	9.48 ± 0.6
	1.0×10^{-4}		23.0 ± 0.6	–	5.8 ± 0.2
E. coli (G^-)	2.5×10^{-3}		33.0 ± 0.8	14.72 ± 0.4	14.5 ± 0.5
	1.0×10^{-3}		30.0 ± 0.5	12.60 ± 0.3	12.3 ± 0.3
	1.0×10^{-4}		20.0 ± 0.6	9.3 ± 0.7	9.6 ± 0.3
S. marcescens (G^-)	2.5×10^{-3}		31.0 ± 0.8	–	9.3 ± 0.7
	1.0×10^{-3}		30.0 ± 0.9	–	5.8 ± 0.2
	1.0×10^{-4}		20.0 ± 0.6	–	2.8 ± 0.2
F-value 1		117.024***	6.563*	2.223^{ns}	23.971***
F-value 2		11.392**	136.659***	7.499***	2.989*
P		0.05	0.05	0.05	0.05

(–) No zone of inhibition; bacteria are resistant to the compounds.
F-value 1: for different bacterial species; F-value 2: for different concentrations of standard drugs, ligand or its Zn complex. Each value is the mean of three reading ± SD.
^{ns}Non-significant, at $p \leq 0.05$ using two-way ANOVA.
*Low significant.
**Medium significant.
***Highly significant.

[Zn(II)-(bhnmab)(sol)] exhibited higher antimicrobial activity than the free ligand (bhnmab), attributed to the adsorption of Zn(II) ions on the surface of the cell wall of microorganisms, disturbing the respiration process of the cell and thus blocking the synthesis of proteins and restricting further growth of the organisms [43, 44]. Accordingly, Zn(II) ions are essential for the growth-inhibition effect. The formation of hydrogen bonds through the azomethine group (C=N) of the complex with the active centers of cell constituents may interfere with normal cell processes [44]. On chelation, the polarity of Zn(II) ions will be reduced due to partial sharing of the positive charge of the zinc ion with donor groups [45, 46].

The differences observed in relative SD of diameter (mm) of the growth inhibition zone of various concentrations of both synthesized compounds and standard drugs were insignificant, confirming the reproducibility of the results (table 2).

4. Conclusion

A new solvatochromic dye (bhnmab) and its Zn complex were synthesized and characterized. The structure of the Zn(II) complex is square pyramidal with an apical ethanol or water. The structure is supported by a CS Chem 3D Ultra Molecular Modeling and Analysis Program. bhnmab exhibited solvatochromic properties in solvents of different polarities and showed high selectivity for DMF. Owing to the red fluorescence emission of [Zn(II)-bhnmab(sol)] at 496 nm in MeCN, it may be used as an advanced material for red light-emitting diode devices. The MW method provides a clean, cheap, and higher yield with less time. *In vitro* comparative studies of inhibition values of bhnmab and its Zn(II) complex revealed that the complex exhibited higher antimicrobial activity than the free ligand (bhnmab) ($P \leq 0.05$).

Acknowledgments

The authors gratefully acknowledge King Abdulaziz University and the Deanship of Scientific Research for financial support (Grant No. 17-013/430), and the authors express their gratitude to the Department of Botany and Microbiology, Faculty of Science, Tanta University, Egypt for providing the great facilities for collecting the test microorganisms required for the biological activity.

References

[1] C.C. Kwok, S.C. Yu, I.H.T. Sham, C.M. Che. *Chem. Commun*., 2758 (2004).
[2] R.W. Begland, W. Del. US 3,962,220 (1976).
[3] J.F. Neumer, H. Del. US 4,002,616 (1977).
[4] K. Shirai, M. Matsuoka, K. Fukunishi. *Dyes Pigm*., **47**, 107 (2000).
[5] S.H. Kim, S.H. Yoon, S.H. Kim, E.M. Han. *Dyes Pigm*., **64**, 45 (2005).
[6] V. Arun, P.P. Robinson, P. Leeju, G. Varsha, V. Digna, K.K.M. Yusuff. *Dyes Pigm*., **82**, 268 (2009).
[7] Y.A. Son, S.Y. Gwon, S.Y. Lee, S.H. Kim. *Spectrochim. Acta, Part A*, **75**, 225 (2010).
[8] S.H. Kim, S.Y. Lee, S.Y. Gwon, Y.A. Son, J.S. Bae. *Dyes Pigm*., **84**, 169 (2010).
[9] S. Wang, S.H. Kim. *Dyes Pigm*., **80**, 314 (2009).
[10] S.H. Zhang, C. Feng. *J Mol. Struct*., **977**, 62 (2010).
[11] K. Serbest, I. Degirmencioglu, Y. Unever, M. Er, C. Kantar, K. Sancak. *J. Organomet. Chem*., **692**, 5646 (2007).
[12] C. Kantar, N. Akdemir, E. Agar, N. Ocak, S. Sasmaz. *Dyes Pigm*., **76**, 7 (2008).
[13] H. Wang, P. Zhao, D. Shao, J. Zhang, Y. Zhu. *J. Struct. Chem*., **20**, 995 (2009).
[14] J. Xie, J. Qiao, L. Wang, J. Xie, Y. Qiu. *Inorg. Chim. Acta*, **358**, 4451 (2005).
[15] N. Raman, S. Ravichandran, C. Thangaraja. *J. Chem. Sci*., **116**, 215 (2004).
[16] S. Parimala, M. Kandaswamy. *Transition Met. Chem*., **29**, 35 (2004).
[17] B.S. Creaven, M. Devereux, A. Foltyn, S. McClean, G. Rosair, V.R. Thangella, M. Walsh. *Polyhedron*, **29**, 813 (2010).
[18] B.K. Singh, A. Prakasha, H.K. Rajourb, N. Bhojakc, D. Adhikaria. *Spectrochim. Acta*, **76**, 376 (2010).

[19] X. Ran, L. Wang, Y. Lin, J. Hao, D. Cao. *Appl. Organomet. Chem.*, **24**, 741 (2010).
[20] N. Raman, A. Sakthivel, R. Jeyamurugan. *Cent. Eur. J. Chem.*, **8**, 96 (2010).
[21] A. Reiss, T. Caproiu, N. Stanica. *Bull. Chem. Soc. Ethiop.*, **23**, 63 (2009).
[22] C. Spinu, M. Pleniceanu, C. Tigae. *Turk. J. Chem.*, **32**, 487 (2008).
[23] L. Li, Y.Q. Dang, H.W. Li, B. Wang, Y. Wu. *Tetrahedron Lett.*, **51**, 618 (2010).
[24] P.G. Lacroix, S.D. Bella, I. Ledoux. *Chem. Mater.*, **8**, 541 (1996).
[25] A. Majumder, G.M. Rosair, A. Mallick, N. Chattopadhyay, S. Mitra. *Polyhedron*, **25**, 1753 (2006).
[26] H.Y. Li, S. Gao, Z. Xi. *Inorg. Chem. Commun.*, **12**, 300 (2009).
[27] CS Chem 3D Ultra Molecular Modeling and Analysis, Cambridge, Available online at: www.cambridgesoft.com (accessed 15 August 2010).
[28] H.T.S. Britton. *Hydrogen Ions*, 4th Edn, pp. 113–114, Chapman & Hall, London (1952).
[29] S.C. Bhangale, V.V. Patil, V.R. Patil. *Inter. J. Pharm. Sci.*, **2**, 39 (2010).
[30] A.L. Barry. *The Antimicrobial Susceptibility Test: Principles and Practices*, p. 163, Lea & Febiger, Philadelphia (1996).
[31] National Committee for Clinical Laboratory Standards. Methods for dilution antimicrobial susceptibility tests for bacteria that grow aerobically. Approved standard M7-A3. National Committee for Clinical Laboratory Standards, Villanova, PA, USA (1993).
[32] W.G. Cochran, G.M. Cox. *Experimental Designs*, 2nd Edn, pp. 293–316, John Wiley, New York (1960).
[33] J.G.R. Martinez, A.S. Valverde, C. Soriano, A. Zehe. *Inorg. Chim. Acta*, **179**, 149 (1991).
[34] J. Xie, J. Qiao, L. Wang, J. Xie, Y. Qiu. *Inorg. Chim. Acta*, **358**, 4451 (2005).
[35] J. Lu, L. Zhang, L. Liu, G. Liu, D. Jia, D. Wu, G. Xu. *Spectrochim. Acta A*, **71**, 1036 (2008).
[36] Y.I. Moharram, I.S. El-Hallag, M.A. El-Attar, M.M. Ghoneim. *Bull. Electrochem.*, **21**, 297 (2005).
[37] M.M. Ghoneim, I.S. El-Hallag, K.Y. El-Baradie, H.S. El-Desoky, M.A. El-Attar. *Monatsh. Chem.*, **137**, 285 (2006).
[38] M.M. Ghoneim, E.M. Mabrouk, A.M. Hassanein, M.A. El-Attar, E.A. Hesham. *Cent. Eur. J. Chem.*, **5**, 898 (2007).
[39] P. Zuman. *The Elucidation of Organic Electrode Process*, pp. 22–24, Academic Press, New York (1969).
[40] R. Greef, R. Peat, L.M. Peter, D. Pletcher, J. Robinson. *Instrumental Methods in Electrochemistry*, p. 187, John Wiley & Sons, New York (1985), Southampton Electrochemistry Group, Ellis Horwood Limited.
[41] Z. Galus. *Fundamentals of Electrochemical Analysis*, p. 238, Wiley, New York (1976).
[42] R.S. Nicholson, I. Shain. *Anal. Chem.*, **36**, 706 (1964).
[43] Y. Anjaneyula, R.P. Rao. *Synth. React. Inorg. Met.-Org. Chem.*, **16**, 257 (1986).
[44] N. Dharmaraj, P. Viswanathamurthi, K. Natarajan. *Transition Met. Chem.*, **26**, 105 (2001).
[45] M.J. Pelczar, E.C.S Chan, N.R. Krieg. *Antibiotics and Other Chemotherapeutic Agents. Microbiology*, 5th Edn, pp. 535–537, Blackwell Science, New York (1998).
[46] T.J. Franklin, G.A. Snow. *Biochemistry of Antimicrobial Action*, 2nd Edn, p. 161, Chapman and Hall, London (1971).